JOURNAL OF MATERIALS SCIENCE **37** (2002) 3595 – 3598

The determination of the critical stress intensity factor in mode II loading and the shear fracture strength of pharmaceutical powder specimens

F. PODCZECK
The School of Pharmacy, University of London, 29/39 Brunswick Square, London, WC1N 1AX, UK
E-mail: fridrun.podczeck@ams1.ulsop.ac.uk

The shear fracture strength and the critical stress intensity factor in mode II loading of lactose monohydrate and acetylsalicylic acid powder compacts has been evaluated. The experimental results of the shear fracture strength and the critical stress intensity factor in mode II loading appeared to be in good agreement with powder behaviour such as lamination and capping during compaction. Values for the critical stress intensity factor in mode II loading depended on the depth of the crack and hence, any reference of such values or their use to calculate a "fracture toughness ratio" (K_{IC}^{I}/K_{IC}^{II}) must refer to the notch depth applied. The results confirmed that the failure of such powder compacts occurs mainly in tension, but that lactose monohydrate has a tendency also to fail in shear. The latter does not apply to acetylsalicylic acid. Hence, lactose monohydrate should only be used cautiously in layer or press-coated tablets.

1. Introduction

The manufacture of tablets is still the most important process in the pharmaceutical industry, as such products are cheap, and the machinery used is highly optimised. However, due to the advancement in therapeutic principles, the character of the drug substances to be compacted is continually changing. This is in contrast to the limited understanding of the physical processes involved in tablet making, as far as the pharmaceutical industry is concerned. Physico-mechanical properties of powders, which determine the compactability of such materials, are rarely evaluated, and the majority of new tablet products are still developed by "trial- and-error" varying excipients until a satisfying formulation has been found.

One key property of pharmaceutical powder compacts is their brittleness [1]. In this respect the tablets are similar to green ceramic bodies or glass specimens. Fracture mechanics should hence be sought to characterise the materials and the compacts. Failure due to crack propagation in brittle specimens can be initiated in three different modes of failure. The first mode ("opening" or "tensile" mode) is, however, the most often encountered one in highly brittle compacts [2]. Shear fracture could occur along weak interfaces, for example, if a preferred particle orientation has taken place during compaction, or if the powder aeration was incomplete during the densification step. The latter could happen on high-speed tablet machinery, if the pre-compression phase was too short. The common production problems related to this failure are lamination and capping. A mode II failure ("sliding" or "in-plane shear" mode) could also be a problem during the manufacture of layer and press-coated tablets. Here, the elastic properties of the opposing sides of the contiguous layers, which may act as plane-crack interface, are non-symmetrical, and the stress field at the tip of the propagating crack will reflect that non-symmetry.

The aim of this paper is to establish the critical stress intensity factor in mode II and the shear fracture stress of pharmaceutical powder specimens, and to relate the findings to the known behaviour of these materials during tabletting. In the pharmaceutical field, such data has not yet been reported.

2. Materials and methods

The following powders were used: Acetylsalicylic acid (ASS, Rütgers Organics GmbH, CF Aubing Pharmaceuticals, Mannheim, Germany, batch 98070230), lactose monohydrate (LM, Borculo Whey Products, Saltney, UK, batch 826704). The particle size was determined using light microscopy (Olympus BH–2, Tokyo, Japan) in connection with image analysis (Seescan Solitaire 512, Cambridge, UK). One thousand particles were inspected, and the mean Feret diameter was determined to be 8.8 ± 4.8 μm and 6.1 ± 3.9 μm for ASS and LM, respectively. The particle density was determined with an air pycnometer (Model 930, Beckman Instruments Inc., USA) and is $1540 \pm 1\,\mathrm{kgm}^{-3}$ and $1400 \pm 2\,\mathrm{kgm}^{-3}$ for LM and ASS, respectively (arithmetic mean and standard deviation of 5 replicates).

The powder specimens were manufactured on an Instron TT universal testing machine (Instron, High Wycombe, UK) at a compaction rate of 1 mm/min,

and on a hydraulic press (Specac 15,000, Specac Ltd., Kent UK). The specimens were compacted to have a thickness of 5 mm after removal from the die. The compaction forces were recorded using a X–Y-recorder (Gould, model 6000, Bryan Southern Ltd., Surrey, UK). Different beam porosities were achieved by varying the specimen weight.

A specially manufactured split-die system was used, which can be dissembled completely, as long as the pressure exerted by the powder compact allows opening. The nominal dimensions of the die are length 45 mm and width 9 mm. A thickness of 5 mm was chosen to have comparable conditions to previous work on mode I and III failure [3, 4]. The nominal volume of the beams is hence 2.025 cm^3. For the calibration experiments (determination of the notch depth for critical stress intensity factor measurements) 30 compacts with a porosity of 0.2 were produced. For all other experiments, 32 (LM) or 36 (ASS) compacts were manufactured, whereby the porosity of the specimens after unloading was between 0.2 and 0.06 (ASS), and between 0.2 and 0.08 (LM).

For the determination of the critical stress intensity factor in mode II loading, K_{IC}^{II}, and the shear fracture strength, τ_f, notches with an opening angle of 90° were inserted into the beams using a miniature file. The notches were measured on both sides using the microscope attached to an image analyser (see above). The magnification was chosen, so that the standard imaging error of 1 pixel resulted in a measuring error of $\pm 5.714\ \mu$m. The calculation algorithm described by [5] was employed to obtain values for the critical stress intensity factor in mode II, and the algorithm described by [1] was utilised to calculate the shear fracture strength.

The breaking load of the beams was obtained on a universal strength tester at a test speed of 1 mm/min (CT–5, Engineering Systems, Nottingham, UK). A four-point bending rig with equal upper and lower span of 30 mm and a horizontal shift of 10 mm was used.

All beams were stored for at least 2 weeks at room temperature (21–24°C) and 40–45% relative humidity of the air. Twenty-four hours before the experiments the specimens were transferred into a desiccator filled with saturated solution of magnesium nitrate (BDH, Poole, UK) i.e., stored under controlled humidity of 53%. Afterwards the specimens were weighed (electronic recording balance, Sartorius, Göttingen, Germany) and measured (electronic callipers; length ± 0.01 mm; width and thickness ± 0.001 mm). The porosity of the specimens was calculated from these data and the density of the materials. The notches were inserted and measured as described above, and the breaking load was determined. All calculations were undertaken using SPSS 9.0 (SPSS Inc, Woking, UK). Non-linear relationships were always treated with non-linear regression to minimise errors when obtaining extrapolations to zero porosity.

3. Results and discussion

3.1. Shear fracture strength

Shear tests on fully plastic materials are normally performed using tube specimens or solid cylindrical bars, which are twisted by a torque loading [6]. However, brittle specimens will fail prematurely in such tests, and hence, alternative loading geometries have been developed, for example, by Iosipescu [7]. Here, rectangular beams with two 90° notches, each having a depth of one quarter of the beam thickness, positioned exactly opposite to each other, are employed. The loading rig (see Fig. 1) provides a horizontal shift between lower and upper loading platform. As a result, the central section of the beam does not experience a bending moment, but a shear force [8]. The shear fracture stress τ_f can be calculated from:

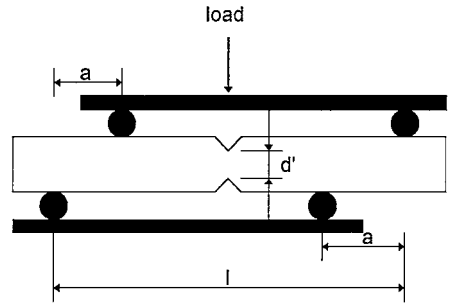

Figure 1 Loading rig for the determination of the shear fracture strength.

$$\tau_f = \frac{F_f a}{b d'(l-a)} \tag{1}$$

where F_f is the fracture load, b is the breadth of the beam, and a, l and d' are defined in Fig. 1.

The determination of the shear fracture strength brought some experimental difficulties because of the large depth of the notches required. Also, the two notches have to be precisely positioned opposite to each other, which requires some skill. A tiny shift of $\pm 5\ \mu$m in horizontal notch position or $\pm 20\ \mu$m in notch depth was found to cause failure due to bending rather than in shear. The former could be detected by observing that other cracks propagated rather than the notches. Beams, which did not fail in shear, were discarded from the results.

The shear fracture strength of the two materials as a function of the beam porosity is compared in Fig. 2. In both cases, the relationship found is exponential in nature. The values for LM are slightly but consistently larger than those obtained for ASS. Extrapolation to zero-porosity in order to establish an estimate for the material shear fracture strength resulted in values of

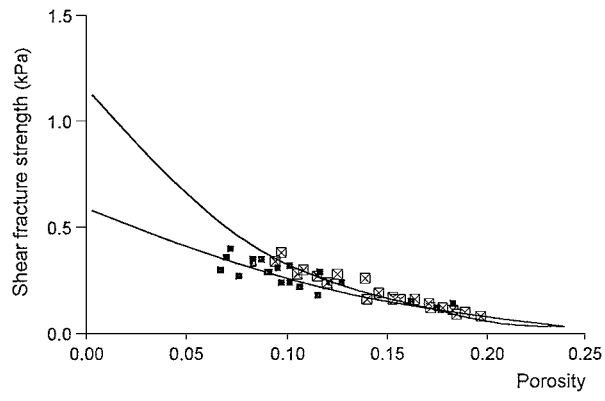

Figure 2 Shear fracture strength as a function of beam porosity for LM (⊠) and ASS (■).

0.63 ± 0.08 kPa ($R^2 = 0.927$, Root-Mean-Square deviation RMS = 6.35%) and 1.20 ± 0.13 kPa ($R^2 = 0.927$, RMS = 1.67%) for ASS and LM, respectively. The shear fracture strength of, for example, LM particles is hence about twice that of ASS particles. The ratio between the yield strengths of these two materials as obtained from out-of-die Heckel-plots was previously found to be of similar magnitude [3]. This implies that shear forces occurring during the compaction process of these powders could have a larger influence on the shape and steepness of the Heckel-functions, and hence on the compactability of the powders. Also, LM compacts are known to be prone to lamination [9], whereas this is not the case for ASS-compacts, when made from fine powder. This suggests that material with a tendency to produce capping or lamination during tabletting can be identified by higher shear fracture strength values.

3.2. Critical stress intensity factor in mode II loading

The determination of the critical stress intensity factor in mode II loading has been rarely reported in the physical literature to date, and is as yet unknown to the pharmaceutical community. A typical test for mode II involves the use of so-called end–notch flexure specimens, which have been notched parallel to the length and breadth of the beam, on one side only [10]. Although the state of the stress at the tip of the crack is a pure shear stress, the method has severe drawbacks in terms of data evaluation [11]. The stress–strain curves in these experiments are non-linear, and it is rather a subjective procedure to extract the required force and deflection information, which would indicate the start of the crack propagation process, from these curves.

The determination of the critical stress intensity factor in mode II loading of rectangular beam specimens with one notch in the middle of the lower beam surface has been described by Dunn *et al.* [5] for Polymethyl methacrylate using a test configuration similar to that shown in Fig. 1. However, here the beams have only one notch at the lower side of the beam. The influence of the notch length on the values has not yet been studied. The advantages of this method over the end-notch flexure technique are the simpler test geometry, in particular with respect to the introduction of the notch into the specimen, and a well-defined end point of the experiment from which exact readings can be obtained. As for the determination of the shear fracture strength, at the tip of the notch the bending moment becomes zero, and a shear force develops. The value for the critical stress intensity factor in mode II loading can be calculated from:

$$K_{\mathrm{IC}}^{\mathrm{II}} = \frac{F_f}{bd}\frac{a_2 - a_1}{a_1 + a_2} d^{1-\lambda} Y \qquad (2)$$

with

$$Y = 10.58\left(\frac{p}{d}\right) + 28.92\left(\frac{p}{2}\right)^2 - 246.64\left(\frac{p}{d}\right)^3 + 518.17\left(\frac{p}{d}\right)^4 - 26.67\left(\frac{p}{d}\right)^5 \qquad (3)$$

where d is the thickness of the beam, λ is the stress singularity factor ($\lambda = 0.9085$ for a notch angle 90°). The values of a_1 and a_2 represent the distances from the mid-point of the notch to the support rolls, whereby $a_2 > a_1$, $a_2 = l/2$ and $a_1 = l/2 - a$.

When measuring the critical stress intensity factor in mode I loading, it was found critical to determine the minimum notch size above which the value of the critical stress intensity factor became independent of this experimental detail [3]. However, in mode III loading using an anti-clastic plate bending method it was found that the value of the critical stress intensity factor decreased steadily with an increase in notch length [4, 12]. In mode III, the stress field in-plane should be pure shear, and hence it can be assumed that also in mode II beam bending techniques, there will be a consistent relationship between notch depth and the value of the critical stress intensity factor. To test this hypothesis, beam specimens of a nominal porosity of 0.2 (0.211 ± 0.004 and 0.228 ± 0.006 for ASS and LM, respectively) were employed. Different notch depth between 35 and 1100 μm were introduced into the lower side of the specimens. The relationships between critical stress intensity factor in mode II loading of such beams and the notch depths are illustrated in Fig. 3. The results confirm the above hypothesis. Hence, values for the critical stress intensity factor in mode II loading can only be presented and compared with strict reference to the notch depth used. The slope of the lines in Fig. 3 is larger for ASS (0.366 ± 0.019, $R^2 = 0.928$, RMS = 5.3%) than for LM (0.205 ± 0.005, $R^2 = 0.982$, RMS = 2.6%). ASS is the more elastic material having a Young's modulus of 1.84 ± 0.03 GPa compared to the value for LM of 2.99 ± 0.06 GPa [3]. Brittle fracture of solids and elasticity are closely related i.e., the method to determine the critical stress intensity factor in mode II loading is derived on the principles of linear elastic fracture mechanics. Thus, the findings from Fig. 3 imply that the method of determination used here is the more sensitive to small variations in notch depth, the more elastic the material tested is. Coincidentally, the ratio between the values of Young's modulus (1.625) is close to the ratio between the values of the slopes of the functions shown in Fig. 3 (1.785).

In previous work [3] a notch depth of 656 ± 62 μm and 865 ± 67 μm for LM and ASS, respectively, was

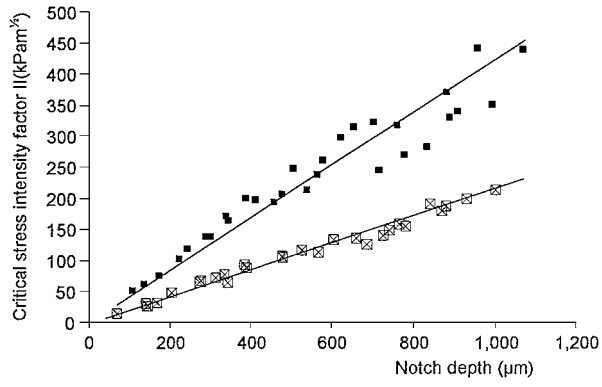

Figure 3 Relationship between critical stress intensity factor in mode II loading and notch depth for beams of a porosity of 0.2 for LM (⊠) and ASS (■).

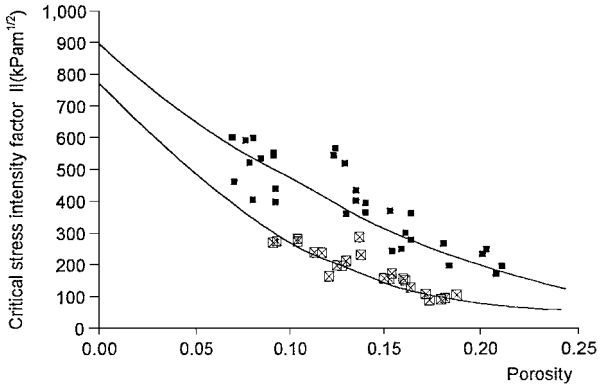

Figure 4 Critical stress intensity factor in mode II loading as a function of the beam porosity for LM (⊠) and ASS (■).

employed to determine the critical stress intensity factor in mode I loading. These notch depths had been chosen so that the resulting values were independent of the notch depth. As such independence, however, appears not to exist for the critical stress intensity factor in mode II loading experiments, the previous values were also set as target notch depths in this work. This renders the possibility of calculating a "fracture toughness ratio" $K^{\mathrm{I}}_{\mathrm{IC}}/K^{\mathrm{II}}_{\mathrm{IC}}$ [13], which can be utilised to determine the likelihood of tensile failure over shear failure, and which is related to the frictional properties of the materials [14]. The experimental average notch depths achieved were 773 ± 68 μm and 908 ± 97 μm for LM and ASS, respectively. These values are slightly larger than those previously used, whereby only the values for LM are statistically significantly different.

In Fig. 4, the critical stress intensity factor in mode II loading as a function of the specimen porosity is compared between ASS and LM. The data are variable, and there is no close fit to the theoretical exponential function linking the two parameters. However, such variability was also observed by Dunn *et al*. [5] and might thus be due to the sensitivity of the loading process to, for example, minute misalignments in the bending rig, or due to small variations in the overall beam thickness. In general, the values obtained for ASS are considerably larger than those observed for LM, which is different from the results of the shear fracture strength. After extrapolation to zero-porosity, the material values for the critical stress intensity factor in mode II loading were found to be 895 ± 85 kPam$^{1/2}$ ($R^2 = 0.721$, RMS = 16.1%) and 771 ± 127 kPam$^{1/2}$ ($R^2 = 0.778$, RMS = 8.4%) for ASS and LM, respectively.

Table I compares the fracture mechanics properties of the two materials. As can be seen, the critical stress intensity factor for different loading modes decreases in the order $K^{\mathrm{III}}_{\mathrm{IC}} \gg K^{\mathrm{II}}_{\mathrm{IC}} > K^{\mathrm{I}}_{\mathrm{IC}}$ for both materials. This confirms the very brittle nature of the specimens, and hence, tensile failure will dominate in most situations. Considering the ratio of $K^{\mathrm{I}}_{\mathrm{IC}}$ over $K^{\mathrm{II}}_{\mathrm{IC}}$, it appears as though LM specimens might, under certain circumstances, also show shear failure, which is in agreement with the results for the shear fracture strength discussed above.

TABLE I Critical stress intensity factors obtained using different loading modes for ASS and LM ($K^{\mathrm{I}}_{\mathrm{IC}}$, critical stress intensity factor in mode I loading, $K^{\mathrm{II}}_{\mathrm{IC}}$, critical stress intensity factor in mode II loading, $K^{\mathrm{III}}_{\mathrm{IC}}$, critical stress intensity factor in mode III loading)

Property	ASS	LM	Reference
$K^{\mathrm{I}}_{\mathrm{IC}}$ (kPam$^{1/2}$)	366 ± 12	493 ± 32	[3]
$K^{\mathrm{II}}_{\mathrm{IC}}$ (kPam$^{1/2}$)	895 ± 85	771 ± 127	
$K^{\mathrm{III}}_{\mathrm{IC}}$ (MPam$^{1/2}$)	$>15.1 \pm 0.8$	102 ± 14	[4]
$K^{\mathrm{I}}_{\mathrm{IC}}/K^{\mathrm{II}}_{\mathrm{IC}}$	0.41	0.64	

4. Conclusions

The work presented provides insight into the possible failure mechanisms of powder compacts and their relative importance. The experimental results of the shear fracture strength and the critical stress intensity factor in mode II loading appear to be in good agreement with powder behaviour during compaction such as lamination and capping. Values for the critical stress intensity factor in mode II loading depend on the depth of the crack and hence, any reference of such values or their use to calculate a "fracture toughness ratio" $K^{\mathrm{I}}_{\mathrm{IC}}/K^{\mathrm{II}}_{\mathrm{IC}}$ must refer to the notch depth applied. The results confirm that the failure of powder compacts will occur mainly in tension, but that LM has a tendency also to fail in shear. The latter does not apply to ASS. Hence, LM should only be used cautiously in layer or press-coated tablets.

Acknowledgements

This work was partly financed by the Deutsche Forschungsgemeinschaft via a Heisenberg–Fellowship. ASS and LM were gifts from Rütgers Organics GmbH, CT Aubing Pharmaceuticals (Mannheim, Germany) and Borculo Whey Products (Saltney, UK), respectively.

References

1. P. STANLEY, *Int. J. Pharm.* **227** (2001) 27.
2. B. LAWN, "Fracture of Brittle Solids," 2nd edn. (Cambridge University Press, Cambridge, UK, 1993) p. 23.
3. F. PODCZECK, *J. Mater. Sci.* **36** (2001) 4687.
4. *Idem*., *Int. J. Pharm.* **227** (2001) 39.
5. M. L. DUNN, W. SUWITO, S. CUNNINGHAM and C. W. MAY, *International Journal of Fracture* **84** (1997) 367.
6. R. HILL, "The Mathematical Theory of Plasticity" (Claredon Press, Oxford, 1998) p. 325.
7. N. IOSIPESCU, *J. Materials* **2** (1967) 537.
8. A. SEERAT-UN-NABI and B. DERBY, *J. Mater. Sci. Lett.* **9** (1990) 63.
9. A. H. DE BOER, H. VROMANS, C. F. LERK, G. K. BOLHIUS and K. D. KUSSENDRAGER, *Pharmaceutical Weekblad* **8** (1986) 145.
10. H. CHAI, *International Journal of Fracture* **37** (1988) 137.
11. *Idem*., *ibid*. **58** (1992) 223.
12. M. FARSHAD and P. FLÜELER, *Engineering Fracture Mechanics* **60** (1998) 597.
13. R. RIKARDS, F.-G. BUCHHOLZ, H. WANG, A. K. BLEDZKI, A. KORJAKIN and H.-A. RICHARD, *ibid*. **61** (1998) 325.
14. K. L. JOHNSON, *Proc. Roy. Soc. London* A **453** (1997) 163.

Received 25 October 2001
and accepted 14 May 2002